Magnetically-Forced Oscillatory Flow over Shallow Topographies

Itoh, Hiroki
Department of Earth System Science and Technology, Interdisciplinary Graduate School of Engineering Sciences, Kyushu University

Honji, Hiroyuki
Department of Earth System Science and Technology, Interdisciplinary Graduate School of Engineering Sciences, Kyushu University

Boyer, Don. L.
Department of Mechanical and Aerospace Engineering, Arizona State University

https://doi.org/10.15017/16596

出版情報：九州大学大学院総合理工学報告. 22 (2), pp.209-214, 2000-09. Interdisciplinary Graduate School of Engineering Sciences, Kyushu University
バージョン：
権利関係：

九州大学大学院総合理工学報告
第22巻 第2号 209 - 214頁 平成12年9月

Engineering Sciences Reports, Kyushu University
(KYUSHU DAIGAKU SOGORIKOGAKU HOKOKU)
Vol. 22, No. 2 pp. 209 - 214 SEPT. 2000

Magnetically-Forced Oscillatory Flow over Shallow Topographies

Hiroki ITOH*, Hiroyuki HONJI** and Don L. BOYER***

(Received 31 May 2000)

Results are described of laboratory and numerical studies of the quasi-2D oscillatory flow over shallow topographies. A periodically oscillatory flow is forced to form magnetically at the center of a shallow water tank, of which the flat bottom floor is incised by a rectangular-cross-sectional straight trough or a V-shaped-cross-sectional straight trough spanning across a width of the tank. The basic flow pattern is an induced steady streaming which consists of four counter-rotating, symmetrical, vortices. The principal effect of a trough is that the streaming over it is constrained to flow closely along its rims, while the symmetry of the four-vortex system is well preserved. The effect of background rotation on the streaming is also explored. The result shows that the symmetry is broken conspicuously of the four-vortex system, in which two cyclonic vortices appear to grow up. Numerically simulated streamline patterns agree qualitatively with the experimental ones for non-rotating cases.

1. Introduction

Streaming flows around various cylindrical obstacles which oscillate periodically in a fluid have been investigated by Schlichting[1], Tatsuno[2)-4)], and others. It is well known that a symmetrical steady streaming is generated around a circular cylinder oscillating normal to its axis. The present paper concerns a similar streaming generated in an oscillatory flow. A novel feature is, however, that the quasi-two-dimensional (2D) primary oscillatory flow is driven by the Lorentz force due to the interaction of a localized magnetic field with an electrolytic current passing through an aqueous solution in a shallow water tank. No submerged rigid obstacles are concerned with this method, which looks promising for its application in the simulation of some quasi-2D geophysical flows. As for this method of fluid driving, a variety of quasi-2D flows have been investigated recently by Ikehata *et al.*[5], Williams *et al.*[6], and others in connection with the studies of stability of 2D vortex systems. By 'quasi-2D' we mean that flows are nearly horizontal because of the shallowness of the fluid layer, though their velocities may vary with depth in the tank. On the other hand, a streaming flow is known to be generated around a submarine canyon when an oscillatory tidal flow prevails over it, as reported in Perenne *et al.*[7]. This gives the underlying motivation for the present work to apply the above-mentioned method of fluid driving to study induced streaming flows over the topographic troughs. By 'trough' we mean here a long narrow hole dug into the surface of a flat bottom floor.

This paper reports some laboratory and numerical results concerning the topographic effects on the streaming flows which are driven by the Lorentz force. In section 2, the experimental procedure is described, and in section 3 the laboratory and numerical results are presented including the photographs of typical flow patterns. Section 4 is devoted to the concluding remarks. This is a sequel to the report for the 9th International Symposium on Flow Visualization (August 2000, Edinburgh).

2. Experimental Procedure

The oscillatory primary flow was driven by the electromagnetic Lorentz force due to the

*Graduate Student, Department of Earth System Science and Technology
**Department of Earth System Science and Technology
***Department of Mechanical and Aerospace Engineering, Arizona State University

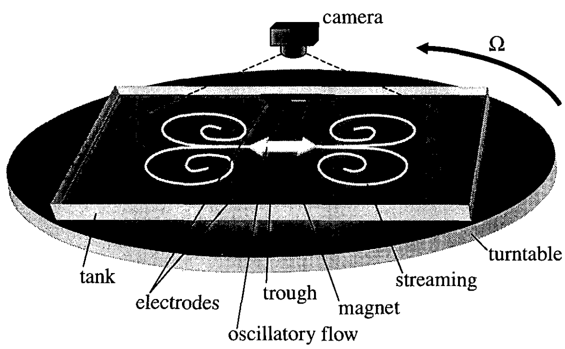

Fig. 1 Experimental setup for non-flat-bottomed, rotating, case.

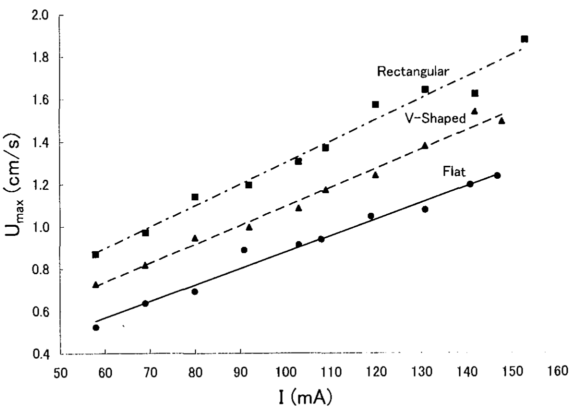

Fig. 2 Electrolytic-current dependence of maximum surface velocities of induced flow at water temperature of 26℃ for three different topographies.

interaction between an electrolytic current passing through a conducting fluid and a localized static magnetic field of a permanent magnet. A typical experimental setup is illustrated in **Fig. 1**, in which Ω indicates the angular velocity of a rotating turntable. A $66 \times 28 \times 3$ cm rectangular water tank filled with a 3 % aqueous solution of sodium carbonate ($NaHCO_3$) serving as the conducting fluid is placed on the turntable with the diameter of 1.0 m. In the experiments, the tank was filled up to the depth of 3.0 mm with the aqueous solution. The otherwise flat bottom-floor of the tank is incised by a rectangular- or V-shaped-cross-sectional straight trough, which spans across the smaller width of the tank through its center. The length, width, and depth of the rectangular trough are 28, 3.0, and 1.0 cm, respectively. A circular permanent magnet with the diameter (d) of 3.0 cm is placed beneath the floor of the tank, and is served as the magnetic field source. The magnitude of the magnetic flux density (B_0) was 0.05 T at the point where the free fluid surface cut across the vertical axis of the magnet. Two brass-rods were submerged in the fluid at both edges of the trough to serve as the electrodes.

When a voltage having the square-wave form with the period of 15 s is applied between the electrodes, an electrolytic current with the magnitude of its density (J_0) passes through the horizontal fluid layer. The typical value of J_0 was taken as 50 mA/cm^2. The interaction of the current with the magnetic field gives rise to the horizontal Lorentz force which drives the fluid in the direction normal to the electric current and the upward oriented magnetic field. The alternating electrolytic current direction generated a primary oscillatory flow over the trough.

The experimental setup above described can be made free from topographies by covering with a thin flat plate, and also free from background rotation by stopping the turntable rotation. Such a flat-bottomed and non-rotating setup has been served as a reference case. In **Fig. 2** are plotted the maximum surface-flow velocities (U_{max}) induced above the center of the magnet, against the applied electrolytic current (I) for three different bottom topographies; flat, V-shaped, and rectangular. The values of U_{max} are used here as characteristic flow velocities (U). When the oscillatory flow continues to prevail, a steady streaming is induced around the localized circular domain of the magnetic field at the center of the tank. The induced streaming flows were visualized by fine tracer particles, which were scattered on the fluid surface and illuminated by two 1kW slide projectors from both sides of the tank. Flow patterns were photographed with a 35 mm camera from above the tank. It should be noted again that the magnetic field is localized and the magnetically-driven primary flows are therefore not spatially uniform in the experiments.

3. Results

The parameters relevant to the streaming patterns are the dimensionless Lorentz force $Q = J_0B_0d/\rho U^2$, the Reynolds number $R = Ud/\nu$, and the Rossby number $Ro = U/\Omega d$, where ρ and ν are the fluid density and kinematic viscosity, respectively. The parameter Q representing the ratio of the Lorentz force to the inertia force is referred also to as the Stuart number [8]. When the floor is incised by the rectangular or V-shaped cross-sectional trough, the streaming pattern depends also on such geometrical parameters as h/w and h/H, where h, w, and H are the depth and width of the trough, and the fluid depth, respectively. In the experiments, h, w, and H were actually kept constant and the dependence of flow patterns on these parameters have not been explored. The values of Uh/ν were less than 115; h/w and h/H were 1/3 and 10/3 in all the experimental runs (As for the V-shaped trough w is the width of its upper opening).

Typical streaming flows for different cases of topography and background rotation are displayed in **Figs. 3－7**, in which each photograph (**a**) is followed by a corresponding schematic illustration (**b**) with arrows indicating flow directions. **Figure 3** (**a**) shows a steady streaming pattern for a flat-bottomed, non-rotating reference case, and (**b**) a schematic illustration of (**a**) where the trajectories of four tracer particles are depicted. The center of the flow field is fitted in the center of the localized circular magnetic field. The primary flow oscillates in the left and right directions, and the streaming is first induced in these directions. As the streaming goes outwards to both directions from the center, however, it turns into one consisting of four counter-rotating symmetrically arranged vortices. Each branch of the streaming returning to the center exhibits a clear zigzag path reflecting the oscillatory motion of the primary flow. The streaming looks quite similar to the one induced around a circular cylinder which is oscillated in fluid at rest. Such a streaming over the flat floor without topography remains almost unchanged when a background rotation is introduced.

A streaming induced over the V-shaped topography is shown in **Fig. 4**, in which (**a**) is a photograph of the streaming and (**b**) its schematic illustration with two straight lines indicating the rims of the V-shaped trough. The streaming pattern still consists of four counter-rotating symmetric vortices, but the return flows coming from outsides to the center are distorted so as to

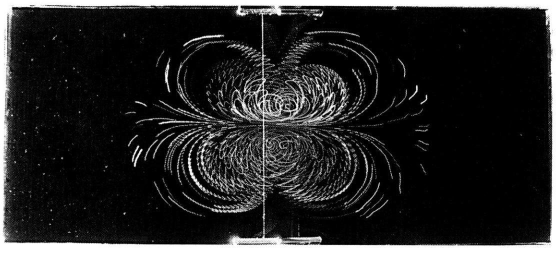

(**a**) Streaming pattern

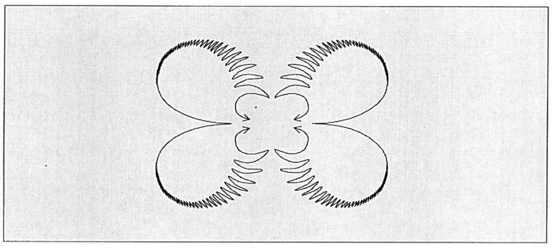

(**b**) Schematic illustration

Fig. 3 Steady streaming pattern for flat-bottomed, non-rotating, reference case at $Q = 5.31$, $R = 345$, and $t_e = 10$ min.

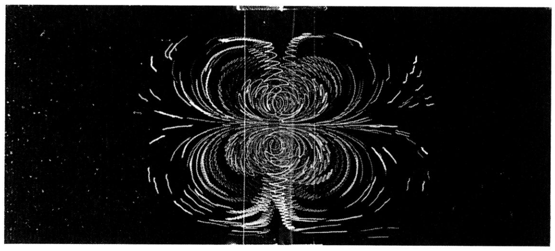

(**a**) Streaming pattern

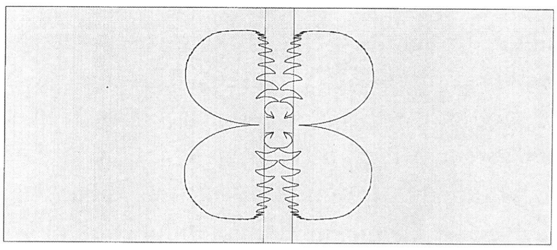

(**b**) Schematic illustration

Fig. 4 Steady streaming pattern for V-shape-bottomed, non-rotating, case at $Q = 4.12$, $R = 345$, and $t_e = 10$ min.

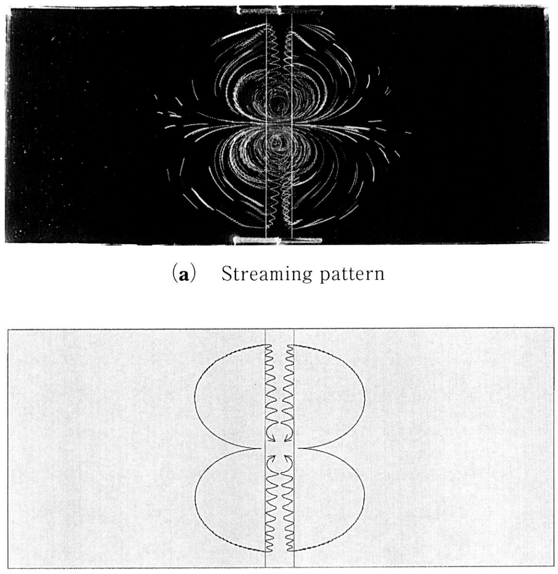

(**a**) Streaming pattern

(**b**) Schematic illustration

Fig. 5 Steady streaming pattern for rectangular-bottomed, non-rotating, case at $Q = 3.26$, $R = 345$, and $t_e = 10$ min.

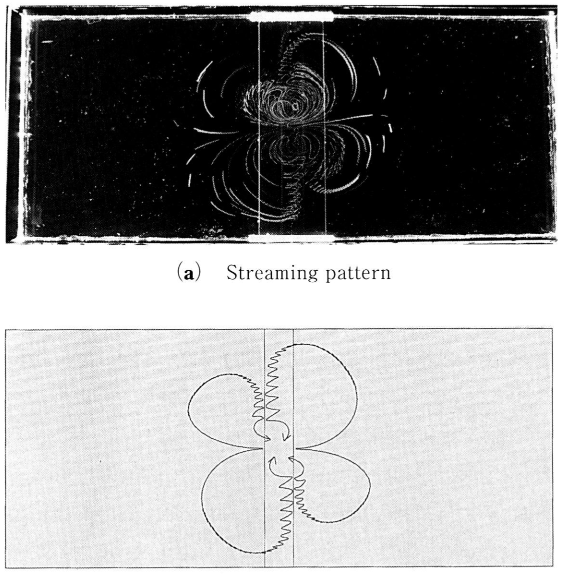

(**a**) Streaming pattern

(**b**) Schematic illustration

Fig. 6 Steady streaming pattern for V-shape-bottomed, rotating, case at $Q = 4.12$, $R = 345$, $Ro = 1.83$ and $t_e = 10$ min.

follow the left and right rims of the trough. This distortion may occur due to the decrease in velocity of the return flow after it passes over the trough rim. When the leftward and rightward streaming flows meet above the trough, they may be organized as a vortex pair that proceeds rapidly towards the center along the rims. Such an effect of the topographic trough is more conspicuous when the bottom floor is incised with the rectangular-cross-sectional straight trough. A streaming induced over the rectangular trough is shown in **Fig. 5**, in which (**a**) shows a photograph of the streaming and (**b**) its schematic illustration with two straight lines indicating the rims of the rectangular trough. Similarly as in the case of **Fig. 4**, the streaming consisting of four symmetric counter-rotating vortices are distorted and the return flows closely follow the rims of the trough. The distortion of the flow pattern in the latter case is more conspicuous than that in the case of **Fig. 4**.

Up to now no background rotation has been considered. When the streaming flows are set up under the influence of background rotation, their symmetric patterns may be distorted depending upon the rotational velocity. A steady streaming pattern over the V-shaped trough with a background rotation being involved is shown in **Fig. 6**, where (**a**) shows a photograph of the streaming and (**b**) its schematic illustration with two parallel lines indicating the trough rims. The symmetry is clearly broken of the streaming, in which the two cyclonic vortices are grown up while the other two anti-cyclonic ones are reduced in size. The streaming associated with the cyclonic vortices returns to the center along the axis of the trough exhibiting a zigzag path. As another example of the rotating case, a streaming over the rectangular-cross-sectional trough is displayed in **Fig. 7**, where (**a**) shows a photograph of the streaming and (**b**) its schematic illustration. From the figure, it is seen that the distortion of the streaming pattern is more conspicuous than in the case of the V-shaped topography in **Fig. 6**. The cyclonic vortices are grown up and the anti-cyclonic ones almost vanish. The reason for asymmetry of the streaming flow could be interpreted as follows. Flowing of the streaming into the trough from shallow flat-floor regions may lead to cyclonic vorticity, except at the center where the streaming direction is outwards from the trough to the shallow regions. In the rotating cases, the Ekman layer thickness is of order 2 mm.

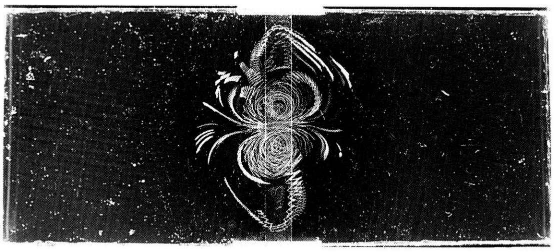

(a) Streaming pattern

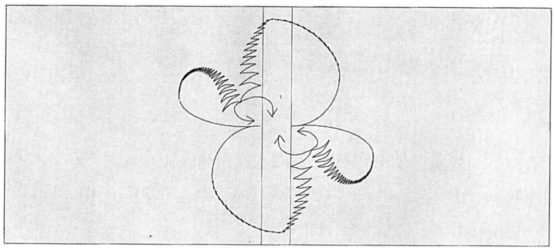

(b) Schematic illustration

Fig. 7 Steady streaming pattern for rectangular bottomed, rotating, case at Q = 3.26, R = 345, Ro = 1.83 and t_e = 10 min.

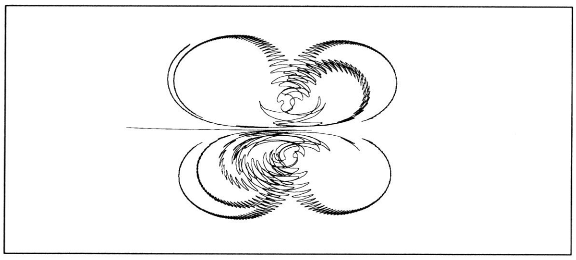

Fig. 8 Computed streaming pattern for flat-bottomed, non-rotating, reference case at Q = 1.00 and R = 500.

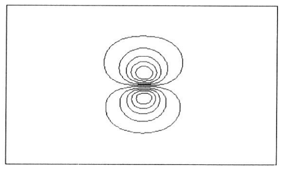

(a) t/T = 0

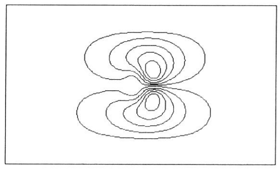

(b) t/T = 15/200

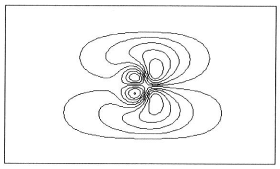

(c) t/T = 18/200

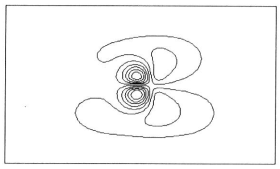

(d) t/T = 21/200

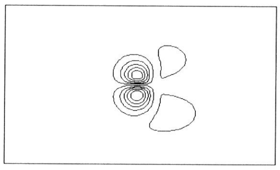

(e) t/T = 24/200

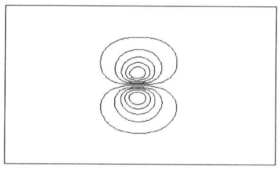

(f) t/T = 0.5

Fig. 9 Streamline patterns at reversion of streaming direction from rightward to leftward at Q = 1.00 and R=500; T is oscillation period and t is elapsed time.

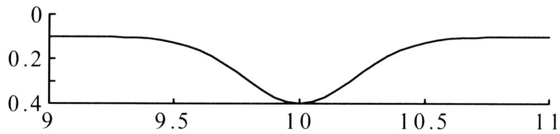

(a) Model topography

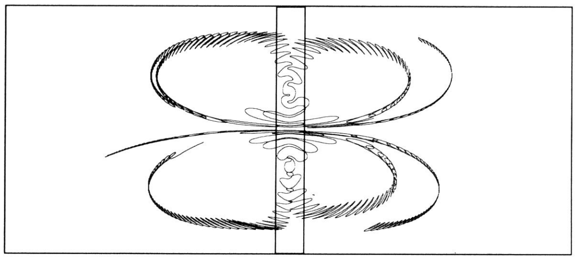

(b) Computed streaming pattern at Q = 1.00 and R = 2.5.

Fig. 10 Streaming over round-V-shaped topography for non-rotating case.

Some numerical results will be presented in the following. The quasi-2D vorticity equation including the so-called Rayleigh term has been used to simulate streaming flows over the flat floor[9]. A computed streaming pattern for a flat-bottomed, non-rotating, reference case is displayed in **Fig. 8**, which is a simulation of the pattern shown in **Fig. 3**. It should be noted here that, in the simulations, Q has been set equal to unity by introducing the representative velocity $(J_0B_0d/\rho)^{1/2}$ and only qualitative features of the streaming flows have been explored preliminarily.

The flow features including the symmetric four vortices and zigzag paths due to the oscillatory motion are well reproduced in the computed figure. Using the same equation, the time-variations of instantaneous streamline patterns have been computed; the result is displayed in **Fig. 9**, in which a process of reversion of the streaming direction during a half period of the oscillatory motion is shown. The symmetry of the vortex is broken as time elapses and recovered at the end; the vortex polarity in **(f)** is reversed from that of **(a)**, however. The above-mentioned equation is not applicable for simulating the flows over three-dimensional topographies. A numerical simulation of the streaming over a round-V-shaped topography is made preliminarily using the vorticity equation [10]. The result is shown in **Fig. 10**, in which the cross-section of the tested topography is shown in (**a**) and the computed streaming pattern in (**b**); the constraint Q = 1 reduced the value of R considerably. Although the topographic shapes are slightly different from each other, this pattern looks quite similar to that shown in **Fig. 4**(**a**); the streaming follows the trough rims and the zigzag paths are well reproduced. Thus, the general features of the streaming over three-dimensional topography can be simulated using the vorticity equation. Numerical studies of the streaming over topographies for rotating cases are being conducted; it is expected that the asymmetry of the streaming will be reproduced properly.

4. Concluding Remarks

A flow visualization study of the streaming flows forced magnetically to set up over shallow topographies including a V-shaped trough and a rectangular trough. The streaming flows under the influence of background rotation have also been investigated.

The main findings are as follows. (1) The steady streaming consisting of four symmetric counter-rotating vortices is formed over such topographies as a flat-floor, a V-shaped trough, and a rectangular trough, when no background rotation is involved. (2) The return flows have a tendency to follow the rims of troughs. (3) When a background rotation is involved, the streaming flows over topographies become asymmetric resulting in grown-up cyclonic vortices. (4) Numerically simulated streaming patterns agree qualitatively with the experimental ones.

We thank Prof. N. Matsunaga, Dr. Y. Sugihara, and Mr. Y. Ikehata for useful discussions. Thanks are also due to Messrs. H. Sakai and H-F. Honji for building an automatic switching device. The support provided by the Japan Society for Promotion of Science is gratefully acknowledged.

References

1) Schlichting, H. : Phys. Z., **33** (1932) 327-335.
2) Tatsuno, M. : J. Phys. Soc. Jpn., **36**, 4 (1974) 1185-1191.
3) Tatsuno, M. : J. Phys. Soc. Jpn., **38**, 1 (1975) 257-264.
4) Tatsuno, M. : Rep. Res. Inst. Appl. Mech., Kyushu Univ., **27**, 85 (1979) 99-110.
5) Ikehata, Y., Honji, H., and Sugihara, Y. : Eng. Sci. Rep., Kyushu Univ., **17**, 4 (1996) 437-442.
6) Benjamin, S. W., Marteau, D., and Gollub, J.P. : Phys. Fluids, **9**, 7 (1997) 2061-2080.
7) Perenne, N., Haidovogel, D.B., and Boyer, D.L. : J. Atm. and Ocean Tech., *in press*.
8) Berger, T.W, Kim, J., Lee, C., and Lim, J. : Phys. Fluids, **12**, 3 (2000) 631-649.
9) Murakami, Y. : Nagare, **13** (1994) 115-123.
10) Van Geffen, J.H.G.M. and Davies, P.A. : Fluid Dyn. Res., **26** (2000) 157-179.